Electronic Supplementary Material (ESI) for Dalton Transactions.


# Supporting Information

## Double layer zinc-UDP coordination polymer: structure and properties

Qi-ming Qiu,[a] Leilei Gu,[a] Hongwei Ma,[b] Li Yan,[b] Minghua Liu[c] and Hui Li*[a]

[a] *Key Laboratory of Cluster Science of Ministry of Education, School of Chemistry and Chemical Engineering, Beijing Institute of Technology, Beijing 100081, P. R. China*
[b] *Analytical and Testing Centre, Beijing Institute of Technology, Beijing 100081, P. R. China*
[c] *Beijing National Laboratory for Molecular Science (BNLMS), CAS Key Laboratory of Colloid, Interface and Chemical Thermodynamics, Institute of Chemistry, Chinese Academy of Sciences, Beijing 100190, P. R. China*

*E-mail: lihui@bit.edu.cn

# Table of Contents

## A. General Methods

**Materials:** All chemical reagents were commercially available and used without further purification. $Zn(NO_3)_2 \cdot 6H_2O$, uridine-5'-diphosphate disodium, 4,4'-bipyridine were purchased from Adamas. Other reagents for fluorescence sensors were purchased from Ark.

**Instrumentation:** FT-IR spectrum was recorded on a Thermo IS5 FT-IR spectrometer using the KBr pellet in the range of 4000–400 $cm^{-1}$. Elemental analyses (C, H, and N) were determined *via* a EA3000 elemental analyzer. $^1H$ NMR, $^1H$-$^1H$ COSY, NOESY and $^{31}P$ NMR spectra were acquired *via* a 400 MHz Bruker Ascend FT-NMR spectrometer using $D_2O$ solvents and the sample was dissolved by heating. X-ray powder diffraction studies were performed by Bruker D8 Advance X-ray diffractometer. The X-ray single crystal data collections were performed on a Bruker SMART CCD diffractometer with graphite monochromatized Mo Kα radiation ($\lambda$ = 0.71073 Å) in 152 K. UV/vis spectra were obtained *via* a TU-1950 spectrophotometer. Fluorescence spectra were obtained at room temperature using a Hitachi F-7000 FL Spectrophotometer with a 450 W xenon lamp as the excitation source. CD measurements were carried out under a constant flow of nitrogen on a JASCO J-810 spectropolarimeter. Thermogravimetric analyses (TGA) were carried out using a DTG-60H thermal analyzer under nitrogen atomosphere from room temperature to 800˚C at the heating rate of 10˚C /min. The SEM images were obtained *via* Hitachi JSM-7500F scanning electron microscopy and the confocal fluorescence images were obtained *via* FV 1000 laser scanning confocal microscopy.

**Experimental details for Heterogeneous fluorescence detection:** The recognition studies of activated **1** (**1a**) were performed at ambient temperature. The recognition ability was studied by adding a fixed amount of different amino acids (Scheme S2) (0.5 mM, in HEPES buffer, pH = 7.4)

to the solid-state **1a** (m = 10 mg). After incubating for 12h, the resulting solution was filtered and then evacuate at 40 ºC for 2 h. The solid-state fluorescence intensity was recorded at $\lambda_{ex}$ = 335 nm and the excitation and emission slits were both set to 2.5 nm.

## B. Syntheses

$\{[Zn(UDP)(4,4'\text{-bipy})(H_2O)_2][Zn_2(UDP)(4,4'\text{-bipy})(H_2O)_6]\cdot 6H_2O\}_n$ (**1**)

An aqueous solution (5 mL) of uridine-5′-diphosphate disodium (UDP·2Na, 22 mg, 0.05 mmol) was added into an aqueous solution (5 mL) of $Zn(NO_3)_2\cdot 6H_2O$ (22 mg, 0.075 mmol). After stirring for 15 min, 4,4′-bipyridine (4,4′-bipy, 8 mg, 0.05 mmol) in distilled water (5 mL) was added to this mixture. The resulting solution was stirred at room temperature for 60 min and then filtered. The colorless block crystals were obtained by evaporation at room temperature after three days. Yield 89%. *Anal*. Calc. (%) for $C_{38}H_{66}N_8Zn_3O_{38}P_4$: C, 29.20; H, 4.26; N, 7.17. Found (%): C, 29.41; H, 4.06; N, 7.39. IR (KBr pallet, $cm^{-1}$): 3382vs, 1676vs, 1608m, 1534w, 1467s, 1412s, 1267m, 1219s, 1146s, 1117s, 1098s, 1047m, 1004w, 922s, 814m, 730m, 670w, 631m, 529m.

## C. Crystal Structure Determination and Refinement

The X-ray single crystal data collection for complex **1** was performed on a Bruker SMART CCD diffractometer with graphite monochromatized Mo Kα radiation ($\lambda$ = 0.71073 Å). Semi-empirical absorption corrections were applied. The structure was solved by direct methods and refined by the full-matrix least-squares method on $F^2$ using the Olex2 and SHELXL programs.[1,2] All non-hydrogen atoms in the complex were refined anisotropically. The hydrogen atoms bound to carbon, nitrogen were located by geometrical calculations, and their positions and thermal parameters were fixed during structure refinement. The hydrogen atoms belonging to water molecules were placed in their geometrically generated positions. Further crystallographic data for structural analyses of complex **1** is summarized in Table S1, selected bond distances and angles with their estimated standard deviations for **1** is summarized in Table S2, and selected H-bonding distances and angles for **1** is summarized in Table S3.

# D. Crystallographic Data and Structural Information

**Table S1.** Crystallographic data for complex **1**.

| Complex | **1** |
|---|---|
| Formula | $C_{38}H_{66}Zn_3N_8O_{38}P_4$ |
| *Mr* | 1562.97 |
| Crystal system | Monoclinic |
| Space group | *C*2 |
| *a* (Å) | 11.1571(16) |
| *b* (Å) | 22.941(3) |
| *c* (Å) | 23.007(4) |
| *α* (°) | 90.00 |
| *β* (°) | 95.972(6) |
| *γ* (°) | 90.00 |
| *V*(Å$^3$) | 5856.8(15) |
| *Z* | 4 |
| F(000) | 3216 |
| Reflections used | 15341 |
| Independent reflections | 10273 |
| Goodness-of-fit on $F^2$ | 1.048 |
| $R_{int}$ | 0.1024 |
| $R_1[I>2\sigma(I)]$ | 0.0429 |
| $wR_2[I>2\sigma(I)]$ | 0.0983 |
| $R_1$(all data) | 0.0558 |
| $wR_2$(all data) | 0.1033 |
| Flack Parameter | 0.005(13) |

**Table S2.** Selected bond distances (Å) and angles (°) for complex **1**.

| | | | |
|---|---|---|---|
| Zn3—O16 | 2.055 (3) | Zn2—O5 | 2.148 (3) |
| Zn3—O16$^{i}$ | 2.055 (3) | Zn2—N2$^{ii}$ | 2.182 (5) |
| Zn3—O15 | 2.157 (3) | Zn2—N3 | 2.190 (6) |
| Zn3—O15$^{i}$ | 2.157 (3) | Zn4—O19 | 2.083 (3) |
| Zn3—N12$^{ii}$ | 2.179 (6) | Zn4—O19$^{vi}$ | 2.083 (3) |
| Zn3—N7 | 2.188 (6) | Zn4—O32$^{vi}$ | 2.124 (3) |
| Zn1—O2 | 2.063 (3) | Zn4—O32 | 2.124 (3) |
| Zn1—O2$^{iii}$ | 2.063 (3) | Zn4—N11 | 2.176 (6) |
| Zn1—N4$^{iv}$ | 2.147 (6) | Zn4—N8$^{iv}$ | 2.189 (6) |
| Zn1—N1 | 2.177 (6) | Zn5—O25 | 2.071 (4) |
| Zn1—O1$^{iii}$ | 2.191 (3) | Zn5—O24 | 2.073 (4) |
| Zn1—O1 | 2.191 (3) | Zn5—O20 | 2.092 (4) |
| Zn2—O4$^{v}$ | 2.092 (3) | Zn5—O26 | 2.116 (4) |
| Zn2—O4 | 2.092 (3) | Zn5—O23 | 2.122 (3) |
| Zn2—O5$^{v}$ | 2.148 (3) | Zn5—O17 | 2.145 (3) |
| P3—O19 | 1.483 (3) | P1—O2 | 1.523 (3) |
| P3—O16 | 1.506 (3) | P1—O6 | 1.638 (3) |
| P3—O17 | 1.521 (4) | P4—O20 | 1.480 (4) |
| P3—O18 | 1.646 (3) | P4—O21 | 1.491 (4) |
| P1—O3 | 1.501 (4) | P4—O22 | 1.583 (4) |
| P1—O4 | 1.509 (3) | P2—O7 | 1.499 (3) |
| P4—O18 | 1.586 (3) | P2—O9 | 1.594 (4) |
| P2—O8 | 1.478 (4) | P2—O6 | 1.600 (4) |
| O16—Zn3—O16$^{i}$ | 176.66 (18) | O4—Zn2—O5 | 89.93 (12) |
| O16—Zn3—O15 | 90.18 (12) | O5$^{v}$—Zn2—O5 | 178.44 (19) |
| O16$^{i}$—Zn3—O15 | 89.78 (12) | O4$^{v}$—Zn2—N2$^{ii}$ | 90.70 (9) |
| O16—Zn3—O15$^{i}$ | 89.78 (12) | O4—Zn2—N2$^{ii}$ | 90.70 (9) |
| O16$^{i}$—Zn3—O15$^{i}$ | 90.18 (12) | O5$^{v}$—Zn2—N2$^{ii}$ | 89.22 (9) |
| O15—Zn3—O15$^{i}$ | 178.67 (19) | O5—Zn2—N2$^{ii}$ | 89.22 (9) |
| O16—Zn3—N12$^{ii}$ | 91.67 (9) | O4$^{v}$—Zn2—N3 | 89.30 (9) |
| O16$^{i}$—Zn3—N12$^{ii}$ | 91.67 (9) | O4—Zn2—N3 | 89.30 (9) |
| O15—Zn3—N12$^{ii}$ | 90.67 (10) | O5$^{v}$—Zn2—N3 | 90.78 (9) |
| O15$^{i}$—Zn3—N12$^{ii}$ | 90.67 (10) | O5—Zn2—N3 | 90.78 (9) |
| O16—Zn3—N7 | 88.33 (9) | N2$^{ii}$—Zn2—N3 | 180.000 (1) |
| O16$^{i}$—Zn3—N7 | 88.33 (9) | O19—Zn4—O19$^{vi}$ | 174.50 (18) |

| | | | |
|---|---|---|---|
| O15—Zn3—N7 | 89.33 (10) | O19—Zn4—O32$^{vi}$ | 86.24 (13) |
| O15$^{i}$—Zn3—N7 | 89.33 (10) | O19$^{vi}$—Zn4—O32$^{vi}$ | 93.81 (13) |
| N12$^{ii}$—Zn3—N7 | 180.0 | O19—Zn4—O32 | 93.81 (13) |
| O2—Zn1—O2$^{iii}$ | 178.25 (18) | O19$^{vi}$—Zn4—O32 | 86.24 (13) |
| O2—Zn1—N4$^{iv}$ | 90.88 (9) | O32$^{vi}$—Zn4—O32 | 178.95 (19) |
| O2$^{iii}$—Zn1—N4$^{iv}$ | 90.88 (9) | O19—Zn4—N11 | 92.75 (9) |
| O2—Zn1—N1 | 89.12 (9) | O19$^{vi}$—Zn4—N11 | 92.75 (9) |
| O2$^{iii}$—Zn1—N1 | 89.12 (9) | O32$^{vi}$—Zn4—N11 | 89.48 (9) |
| N4$^{iv}$—Zn1—N1 | 180.000 (1) | O32—Zn4—N11 | 89.48 (9) |
| O2—Zn1—O1$^{iii}$ | 85.40 (12) | O19—Zn4—N8$^{iv}$ | 87.25 (9) |
| O2$^{iii}$—Zn1—O1$^{iii}$ | 94.67 (12) | O19$^{vi}$—Zn4—N8$^{iv}$ | 87.25 (9) |
| N4$^{iv}$—Zn1—O1$^{iii}$ | 87.50 (9) | O32$^{vi}$—Zn4—N8$^{iv}$ | 90.52 (9) |
| N1—Zn1—O1$^{iii}$ | 92.50 (9) | O32—Zn4—N8$^{iv}$ | 90.52 (9) |
| O2—Zn1—O1 | 94.67 (12) | N11—Zn4—N8$^{iv}$ | 180.0 |
| O2$^{iii}$—Zn1—O1 | 85.40 (12) | O25—Zn5—O24 | 89.92 (15) |
| N4$^{iv}$—Zn1—O1 | 87.50 (9) | O25—Zn5—O20 | 174.93 (16) |
| N1—Zn1—O1 | 92.50 (9) | O24—Zn5—O20 | 94.40 (15) |
| O1$^{iii}$—Zn1—O1 | 175.00 (17) | O25—Zn5—O26 | 92.24 (19) |
| O4$^{v}$—Zn2—O4 | 178.59 (18) | O24—Zn5—O26 | 82.81 (15) |
| O4$^{v}$—Zn2—O5$^{v}$ | 89.93 (12) | O20—Zn5—O26 | 85.69 (19) |
| O4—Zn2—O5$^{v}$ | 90.08 (12) | O25—Zn5—O23 | 89.70 (14) |
| O4$^{v}$—Zn2—O5 | 90.08 (12) | O24—Zn5—O23 | 93.28 (13) |
| O24—Zn5—O17 | 176.19 (13) | O20—Zn5—O23 | 92.69 (15) |
| O20—Zn5—O17 | 88.70 (15) | O26—Zn5—O23 | 175.63 (17) |
| O26—Zn5—O17 | 95.24 (15) | O25—Zn5—O17 | 86.88 (14) |
| O23—Zn5—O17 | 88.78 (13) | | |

Symmetry codes: (i) −*x*, *y*, −*z*; (ii) *x*−1/2, *y*−1/2, *z*; (iii) −*x*+2, *y*, −*z*+1; (iv) *x*+1/2, *y*−1/2, *z*; (v) −*x*+1, *y*, −*z*+1; (vi) −*x*+1, *y*, −*z*.

**Table S3.** Selected H-bonding distances (Å) and angles (°) for complex **1**.

| D–H | d(D–H) | d(H···A) | ∠DHA | d(D···A) | A | Symmetry |
|---|---|---|---|---|---|---|
| N6–H6A (n) | 0.88 | 1.91 | 174 | 2.79 | O3 (βp ) | [ $x$ – 1/2, $y$ – 1/2, $z$ ] |
| N10–H10 (n) | 0.88 | 2.04 | 171 | 2.91 | O17 (βp) | [ $x$ – 1/2, $y$ + 1/2, $z$ ] |
| O15–H15B (cw) | 0.85 | 2.07 | 142 | 2.79 | O19 (βp) | [ –$x$, $y$, –$z$ ] |
| O32–H32A (cw) | 0.85 | 1.92 | 154 | 2.71 | O30 (n) | [ $x$ + 1/2, $y$ – 1/2, $z$ ] |
| O25–H25B (cw) | 0.85 | 1.95 | 160 | 2.77 | O31 (n) | [ $x$ + 1/2, $y$ – 1/2, $z$ ] |
| O26–H26A (cw) | 0.89 | 1.83 | 154 | 2.65 | O16 (βp) | |
| O24–H24A (cw) | 0.85 | 1.79 | 167 | 2.63 | O3 (βp) | [ $x$ – 1/2, $y$ – 1/2, $z$ ] |
| O25–H25A (cw) | 0.85 | 1.86 | 175 | 2.71 | O8 (αp) | [ $x$ – 1/2, $y$ – 1/2, $z$ ] |
| O15–H15A (cw) | 0.85 | 2.38 | 148 | 3.14 | O36 (fw) | [ $x$ – 1, $y$ , $z$ ] |
| O24–H24B (cw) | 0.85 | 2.42 | 139 | 3.11 | O34 (fw) | [ $x$ – 1/2, $y$ – 1/2, $z$ ] |
| O33–H33A (fw) | 0.85 | 2.05 | 168 | 2.89 | O7 (αp) | [ –$x$ + 2, $y$ , –$z$ + 1 ] |
| O33–H33B (fw) | 0.85 | 2.10 | 168 | 2.94 | O35 (fw) | [ –$x$ + 1, $y$ , –$z$ + 1 ] |
| O34–H34A (fw) | 0.88 | 2.02 | 172 | 2.89 | O4 (αp) | |
| O34–H34B (fw) | 0.85 | 1.91 | 173 | 2.75 | O28 (h) | |
| O35–H35A (fw) | 0.85 | 1.99 | 154 | 2.78 | O11 (h) | [ –$x$ + 1, $y$ , $z$ ] |
| O36–H36A (fw) | 0.82 | 1.84 | 175 | 2.65 | O26 (cw) | [ $x$ + 1, $y$ , $z$ ] |
| O37–H37A (fw) | 0.85 | 2.17 | 148 | 2.93 | O12 (n) | |
| O37–H37B (fw) | 0.86 | 2.02 | 161 | 2.85 | O15 (cw) | [ $x$ + 1, $y$ , $z$ ] |
| O38–H38A (fw) | 0.85 | 1.95 | 166 | 2.78 | O5 (cw) | |

(cw) refers to coordinated water. (fw) refers to free water.

(αp) refers to α-oygen on the phosphate group. (βp) refers to β-oygen on the phosphate group.

(n) refers to nucleobase. (h) refers to ribose hydroxyl.

## Supporting information of nucleotide ligand

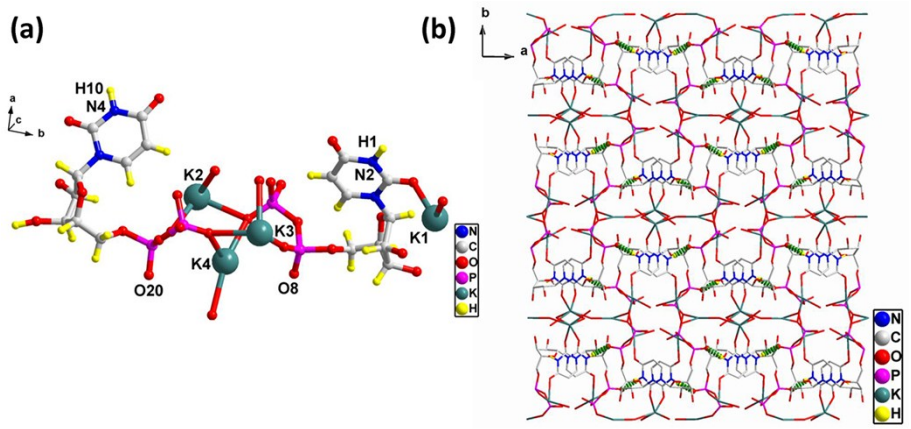


**Fig. S1.** (a) Molecular structure of $UDP^{2-}{\cdot}2K^{+}{\cdot}3H_2O$. (b) The stacking structure of $UDP^{2-}{\cdot}2K^{+}{\cdot}3H_2O$ along the *c* axis. Cif data obtained from the ref. [3] with permission.

## Supporting information of amino acids for fluorescence detection experiment

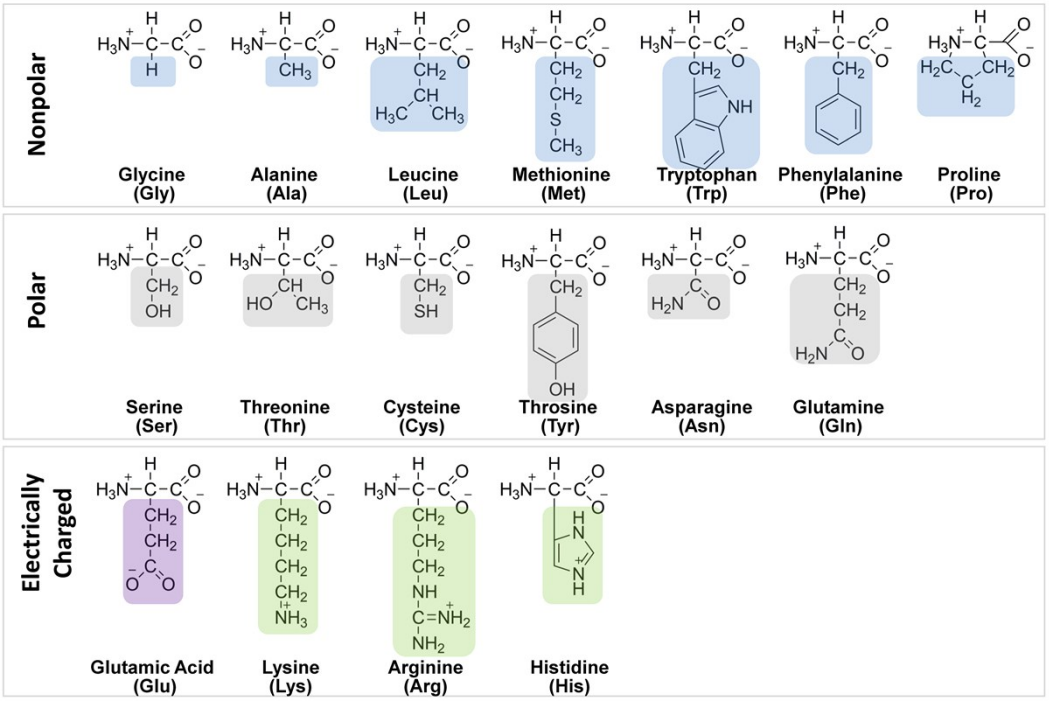


**Scheme S1.** Structural scheme of 17 common α-amino acids used in this research.

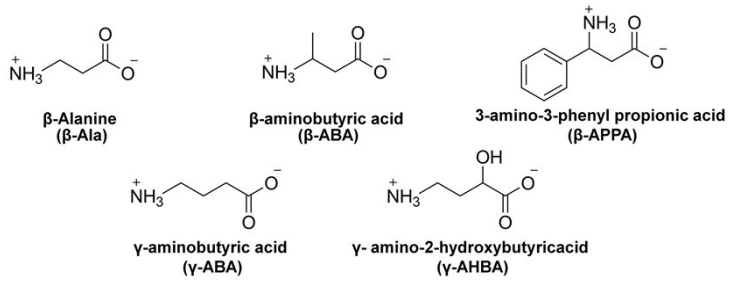


**Scheme S2.** Structural scheme of five β-/γ- amino acids used in this research.

**Supporting information of complex 1**

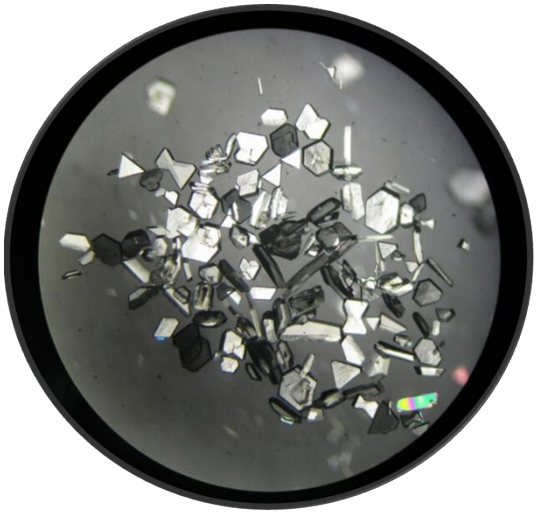

**Fig. S2.** Image of complex **1**.

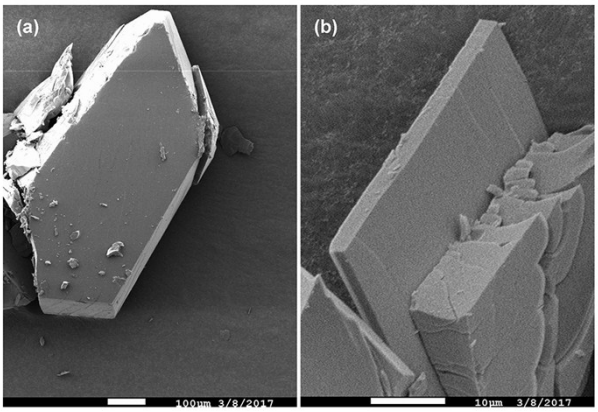


**Fig. S3.** SEM image of complex **1**.

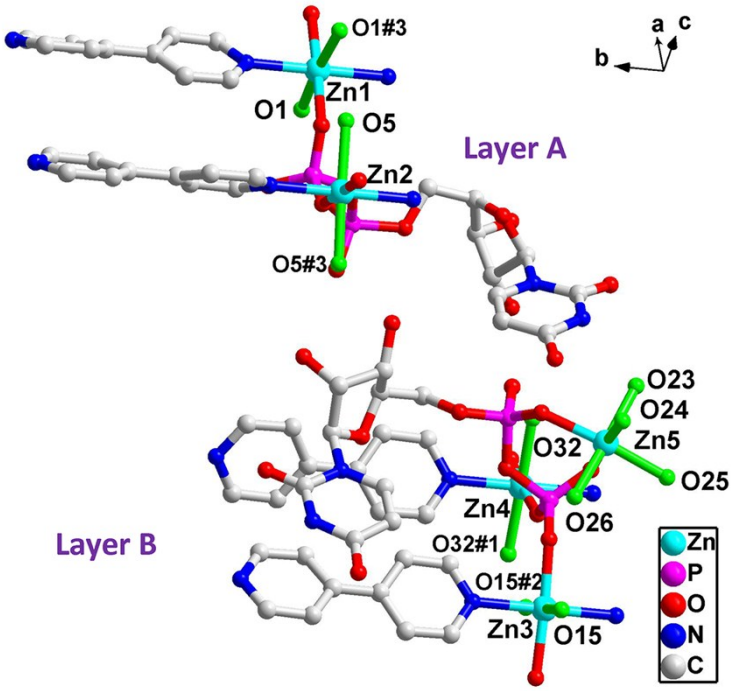


**Fig. S4.** Molecular structure of complex **1**. The complex consists of layer **A** and **B** and the hydrogen atoms are not shown for clarity. Symmetry codes: (#1) −*x*+1, *y*, −*z*; (#2) −*x*, *y*, −*z*; (#3) −*x*+2, *y*, −*z*+1; (#4) −*x*+1, *y*, −*z*+1.

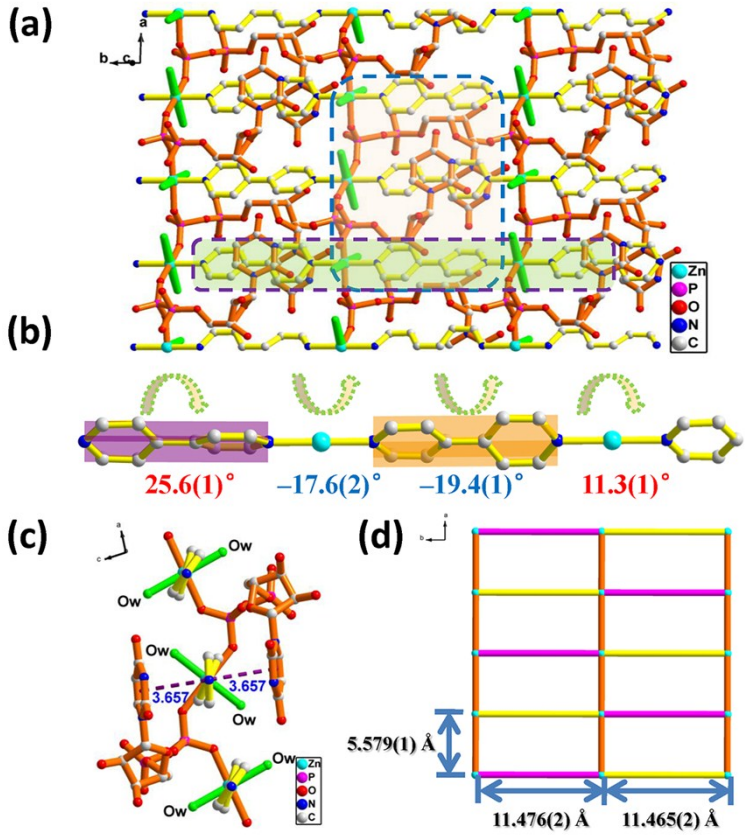


**Fig. S5.** (a) 2D sheet of $\{[Zn(UDP)(4,4'\text{-bipy})(H_2O)_2]\}_n^{n-}$ layer **A**, the coordinated water molecules are highlight with green color. (b) Structural picture of 1D chiral chain of layer **A** generated from Zn–L coordination and inducement of chiral nucleotides. The two pyridine rings of 4,4'-bipy are non-coplanar with dihedral angles of 25.1(6)° and –19.4(1)° respectively, the π–π stacking interaction as well as coordination interaction through $Zn^{II}$ lead the adjacent 4,4'-bipy are also non-coplanar with dihedral angles of –17.6(2)° and 11.3(1)° respectively. (c) π–π stacking interactions between uracil base and pyridine (Purple dashed lines). (d) 2D topology sheet of layer **A** formed by 4,4′-bipy-Zn(II)-4,4′-bipy and phosphate-Zn(II)-phosphate chains.

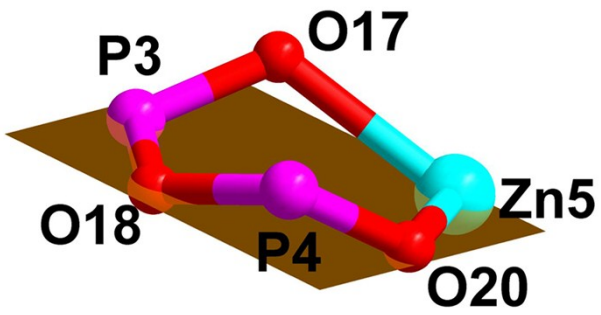


**Fig. S6.** The boat conformation of the six-member coordination ring formed by Zn5 and diphosphate group.

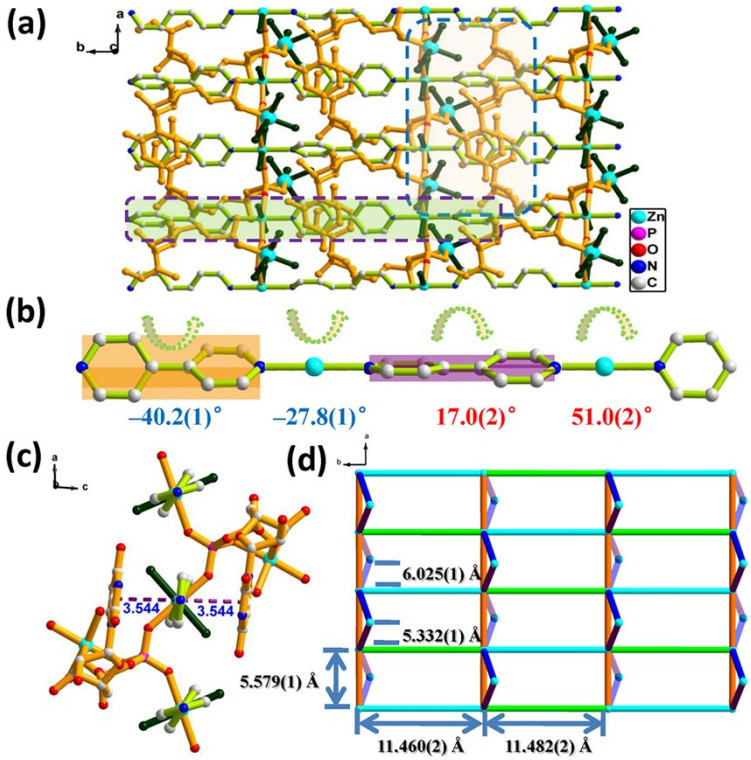


**Fig. S7.** (a) 2D sheet of $\{[Zn_2(UDP)(4,4'\text{-bipy})(H_2O)_6]\}_n^{n+}$ layer **B**, the coordinated water molecules are highlight with dark green color. (b) Structural picture of 1D chiral chain of layer **B** generated from Zn–L coordination and inducement of chiral nucleotides. (c) π–π stacking interactions between uracil base and pyridine (Purple dashed lines). (d) 2D topology sheet of layer **B** formed by 4,4′-bipy-Zn(II)-4,4′-bipy, phosphate-Zn(II)-phosphate chains and chelating coordination ring.

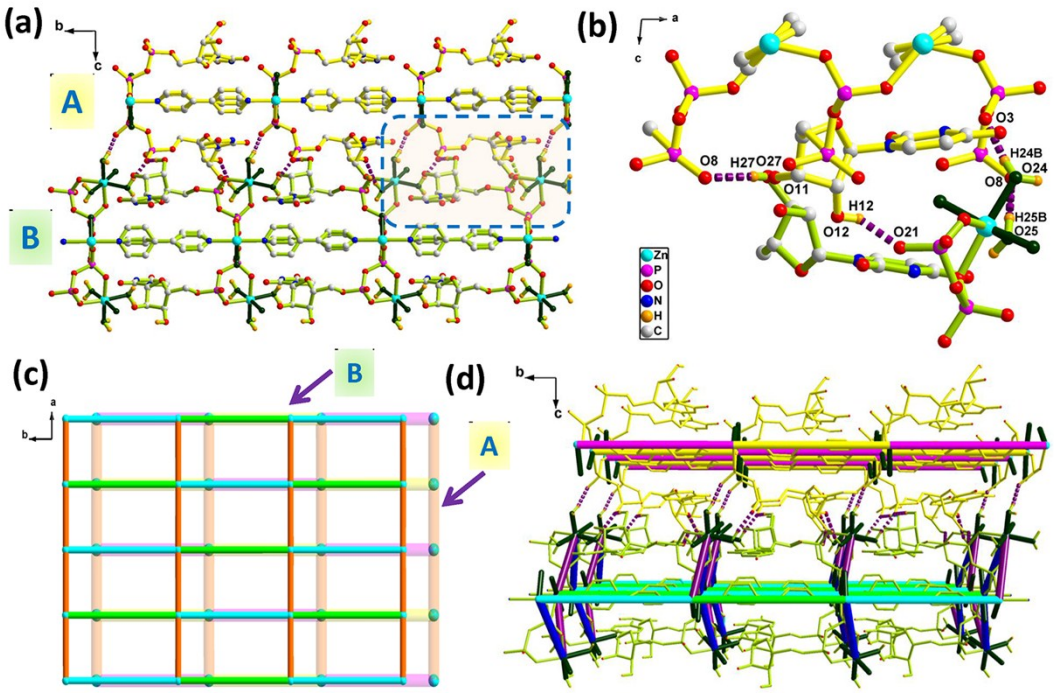


**Fig. S8.** (a, b) Layer **A** (yellow bond) and **B** (green bond) are stabilized by O–H···O H-bonding among coordinated water, diphosphate and hydroxyl (O–H···O, 1.79–1.91 Å, 2.55–2.71 Å, 139–175°). , The coordinated water molecules are highlight with dark green color. (c) The relationship between 2D topology sheet of layer **A** and **B**. (d) Perspective picture along *a* axis, each topology sheet is connected by abundant O–H···O H-bonding among coordinated water, diphosphate and hydroxyl.

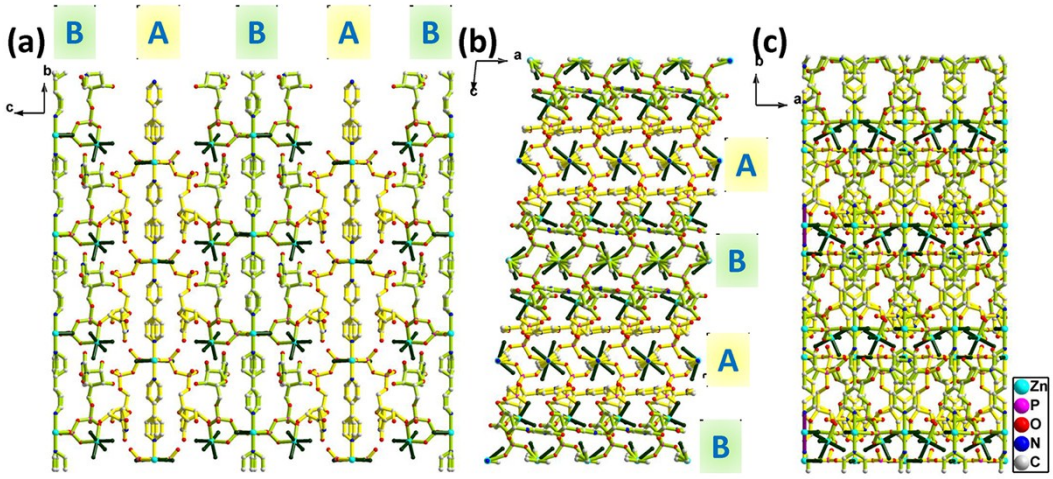


**Fig. S9.** The 3D supramolecular structure of **1** assembled by Layer **A** and **B** from *a*, *b* and *c* axis, respectively.

**The two different definitions of conformation of diphosphate:** Torsion angle Θ: $P_{\alpha}$–$O_{bridging}$–$P_{\beta}$–O

1. In spectroscopic and crystallographic publications, the notation *cis* (~ 0°), *trans* (~ 180°), ±*gauche* (~ ± 60°) is most frequently employed.[4]
   (1) −30°~30° *cis*
   (2) −90°~−30° −*gauche*
   (3) +90°~+30° +*gauche*
   (4) −180°~−150° *trans*
   (5) +180°~+150° *trans*

2. The ranges commonly used in organic chemistry are those proposed by Klyne and Prelog, *viz*. *syn* (~ 0°), *anti* (~ 180°), ±*synclinal* (~ ± 60°) and ±*anticlinal* (~ ± 120°). As the IUPAC-IUB subcommission on nucleotide nomenclature has recommended the KlynePrelog torsion angle ranges, these will be used throughout this text. [4–7]
   (1) −30°~30° *syn*
   (2) −90°~−30° −*synclinal*
   (3) +90°~+30° +*synclinal*
   (4) −150°~−90° −*anticlinal*
   (5) +150°~+90° +*anticlinal*
   (6) −180°~−150° *anti*
   (7) +180°~+150° *anti*

**The definition of conformation of glycosidic bond:** the conformation corresponds to a C2–N1–C1'–O4' torsion angle (Scheme S1). The *high-anti* (-*sc*) range with $\chi \sim -90°$ is actually part of *syn* and the *high-syn* range is part of *anti*, *ac*. [4]
   (1) −90°~90° *syn*
   (2) −90°~−60° *high-anti*, −*sc*
   (3) +180°~+90° *anti*, *ac*
   (4) −180°~−90° *anti*, −*ac*
   (5) +120°~+90° *high-syn*

**Table S4.** Summary of similarities and differences of $\{[Zn(UDP)(4,4'\text{-bipy})(H_2O)_2]\}_n^{n-}$ (layer **A**), $\{[Zn_2(UDP)(4,4'\text{-bipy})(H_2O)_6]\}_n^{n+}$ (layer **B**).

| | layer **A** | layer **B** |
|---|---|---|
| Zn−$O_{phosphate}$ bond distance | 2.063(3) −2.092(3) Å | 2.055(3) −2.145(3) Å |
| Zn−$O_{water}$ bond distance | 2.148(3) −2.191(3) Å | 2.071(4) −2.157(3) Å |
| Zn−$N_{bipy}$ bond distance | 2.147(6) −2.190(6) Å | 2.176(6) −2.189(6) Å |
| Zn···Zn distance | 11.476(2) Å, 11.465(2) Å<br>5.579(1) Å | 11.460(2) Å, 11.482(2) Å,<br>5.579(1) Å<br>5.332(1) Å, 6.025(1) Å |
| π–π stacking interaction | 3.657(3) Å | 3.544(3) Å |
| P−O−P bond angles | 129.2(2)° | 127.3(2)° |
| Dihedral angles in 4,4′-bipy molecule | 25.1(6)°, −19.4(1)°<br>−17.6(2)°, 11.3(1)° | −40.2(1)°, 17.0(2)°<br>−27.8(1)°, 51.0(2)° |
| Bridging ligand | Phosphate group / 4,4′-bipy | Phosphate group / 4,4′-bipy |
| Chelating ligand | – | Phosphate group |
| Dimension | 2 | 2 |
| **Conformations** | | |
| diphosphate | P2–O6–P1–O2 –145.4(2)° *–anticlinal*<br>P2–O6–P1–O4 98.0(3)° *+anticlinal*<br>P2–O6–P1–O3 –24.0(3)° *syn* | P4–O18–P3–O19 –123.0(3)° *–anticlinal*<br>P4–O18–P3–O16 119.2(3)° *+anticlinal*<br>P4–O18–P3–O17 0.6(3)° *syn* |
| glycosidic bond | C21–N5–C17–O10 –120.6(5)° *anti, –ac* | C33–N9–C32–O29 –148.3(5)° *anti, –ac* |

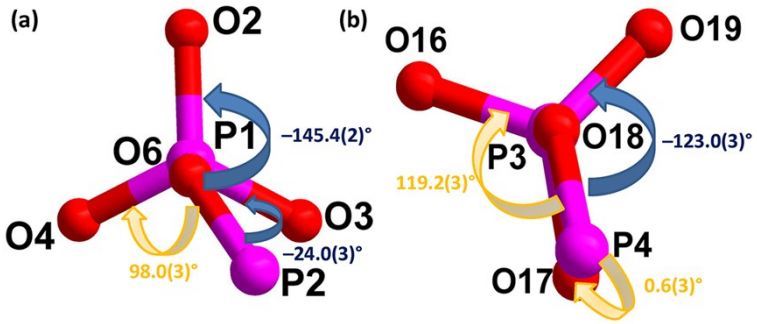


**Fig. S10.** Definition of torsion angles of diphosphate. (a) In layer **A**: torsion angle θ (P2–O6–P1–O3/O2/O4) describing orientations of bonds P2–O6 and P1–O3/O2/O4 with respect to the central bond O6–P1. (b) In layer **B**: torsion angle θ (P4–O18–P3–O16/O17/O19) describing orientations of bonds P4–O18 and P3–O16/O17/O19 with respect to the central bond O18–P3.

## E. PXRD Patterns

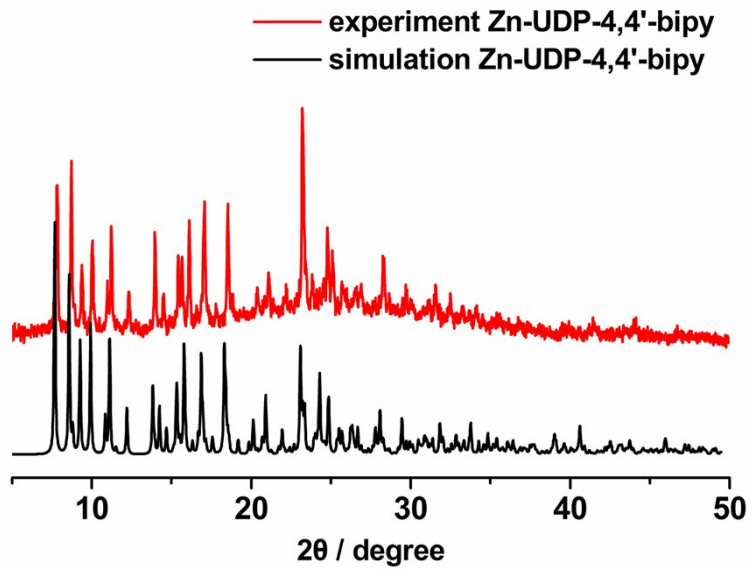


**Fig. S11.** PXRD patterns show the comparison between the experimental value and calculated ones for complex **1**. The phase purity of **1** is confirmed by PXRD.

## F. IR Spectra

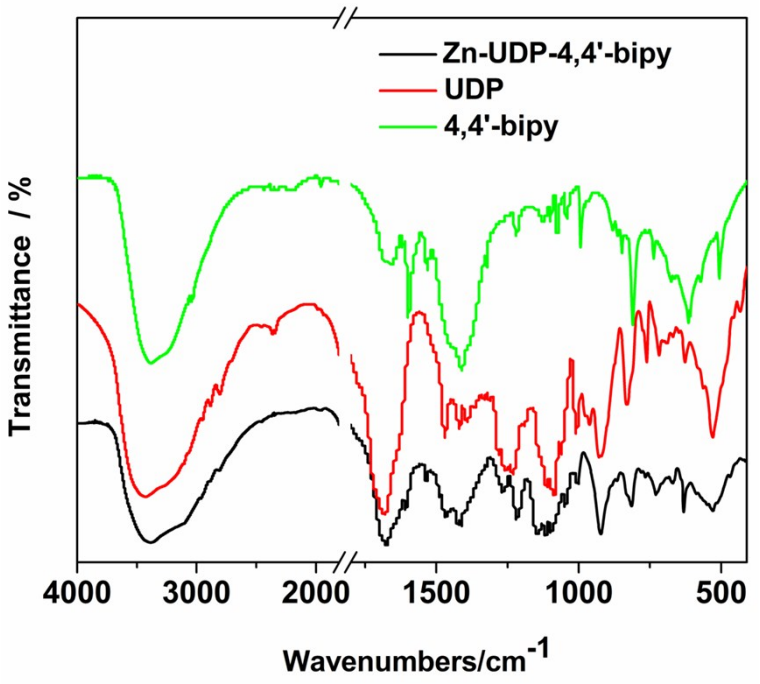


**Fig. S12.** IR spectra of UDP, 4,4′-bipy and complex **1**.

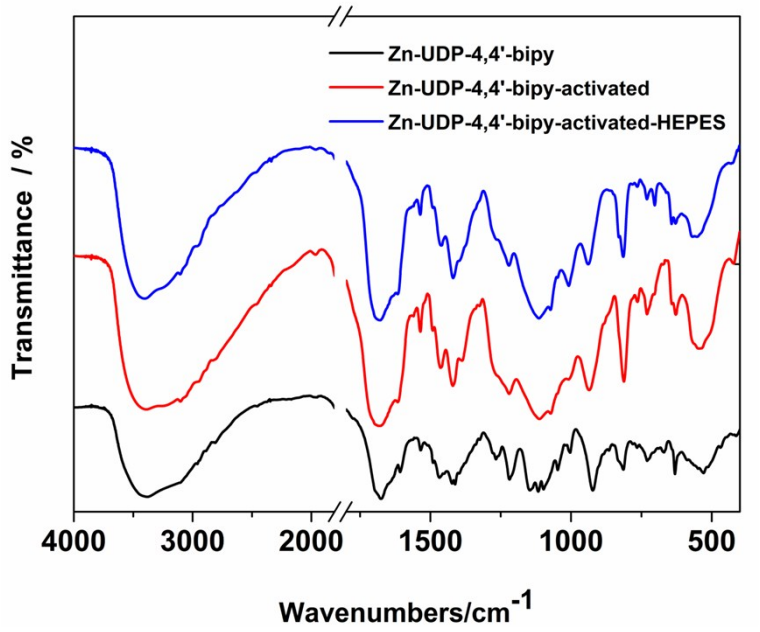


**Fig. S13.** IR spectra of complex **1**, **1a** and **1a** soaking with HEPES buffer (pH = 7.4).

## G. $^{1}$H NMR and $^{31}$P NMR

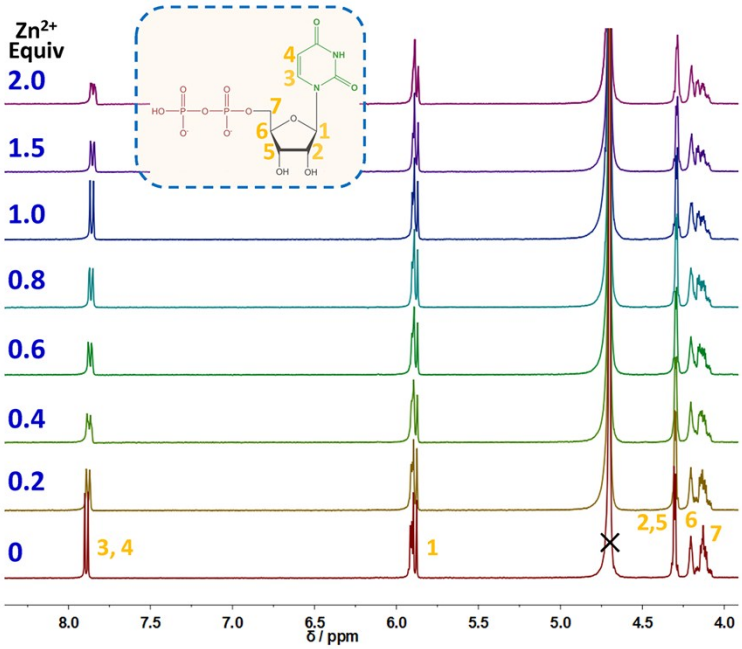


**Fig. S14.** $^{1}$H NMR spectra (400 MHz, 298 K, $D_2O$) of UDP in the presence of the $Zn(NO_3)_2$ titration at different concentrations. The significant chemical shifts of protons suggest that the $Zn^{2+}$ is coordinated to UDP.

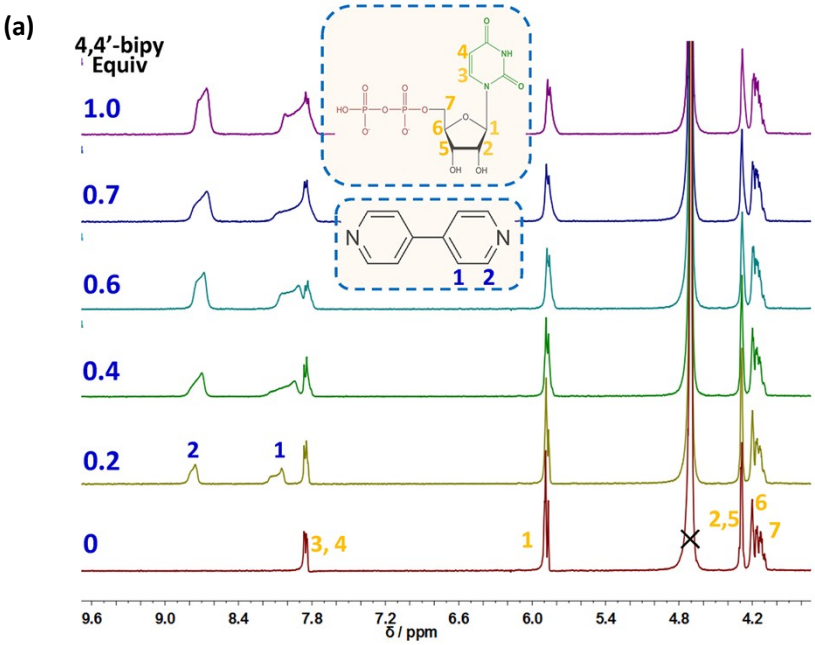

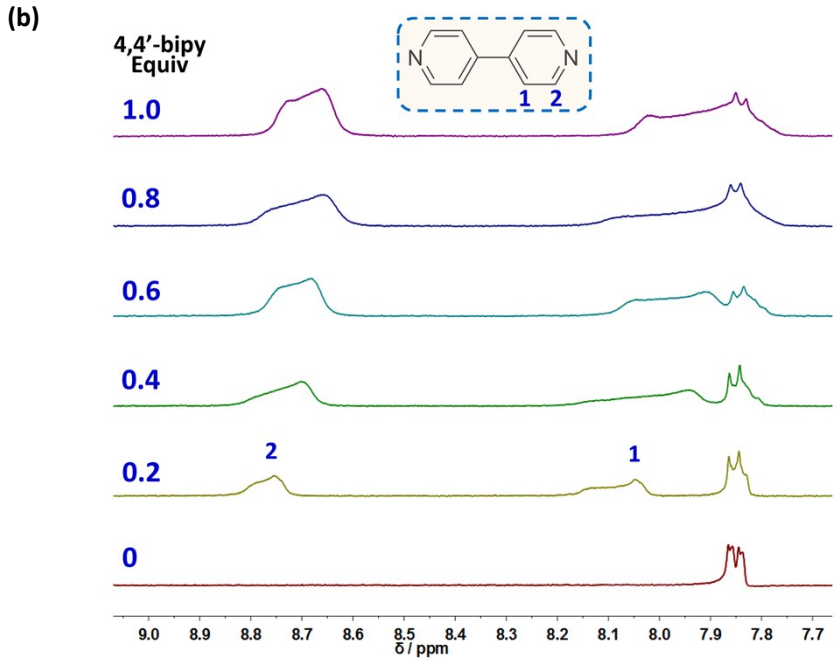


**Fig. S15** (a) $^{1}$H NMR spectra (400 MHz, 298 K, $D_2O$) of Zn-UDP in the presence of the 4,4′-bipy titration at different concentrations. (b) $^{1}$H NMR spectra showed significant chemical shift changes in the resonances for the H-1 and H-2 protons of 4,4′-bipy.

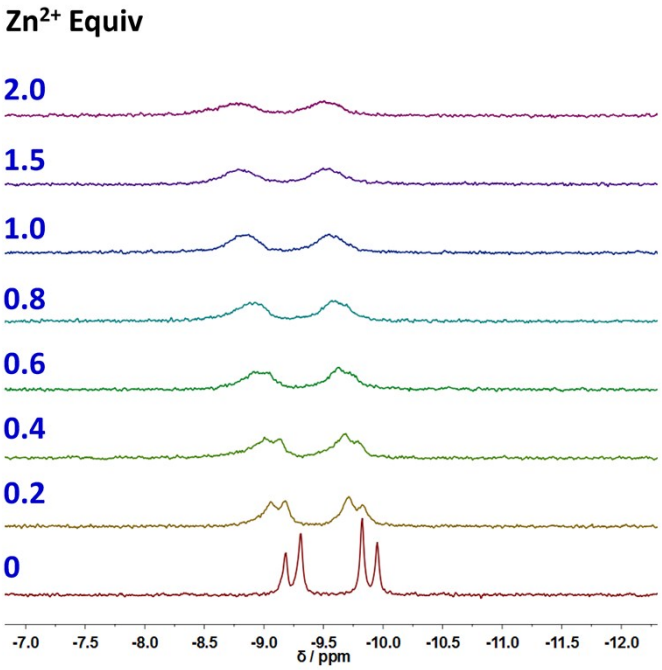


**Fig. S16.** $^{31}$P NMR spectra of UDP in the presence of the $Zn(NO_3)_2$ titration at different concentrations. The significant chemical shifts of phosphorus and gradually weakened of absorption peaks around –10.0 ~ –8.8 ppm suggest that the $Zn^{2+}$ is coordinated to the phosphate of UDP.

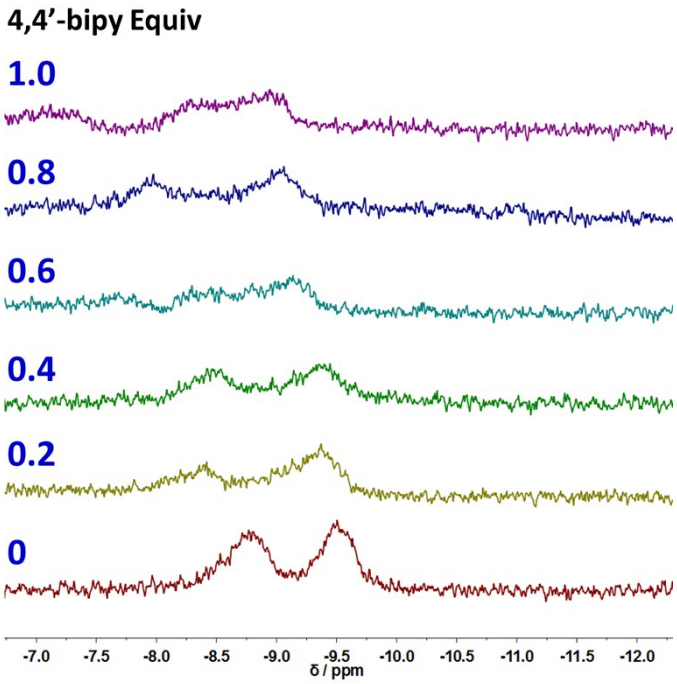


**Fig. S17.** $^{31}$P NMR spectra of Zn-UDP in the presence of the 4,4′-bipy titration at different concentrations.

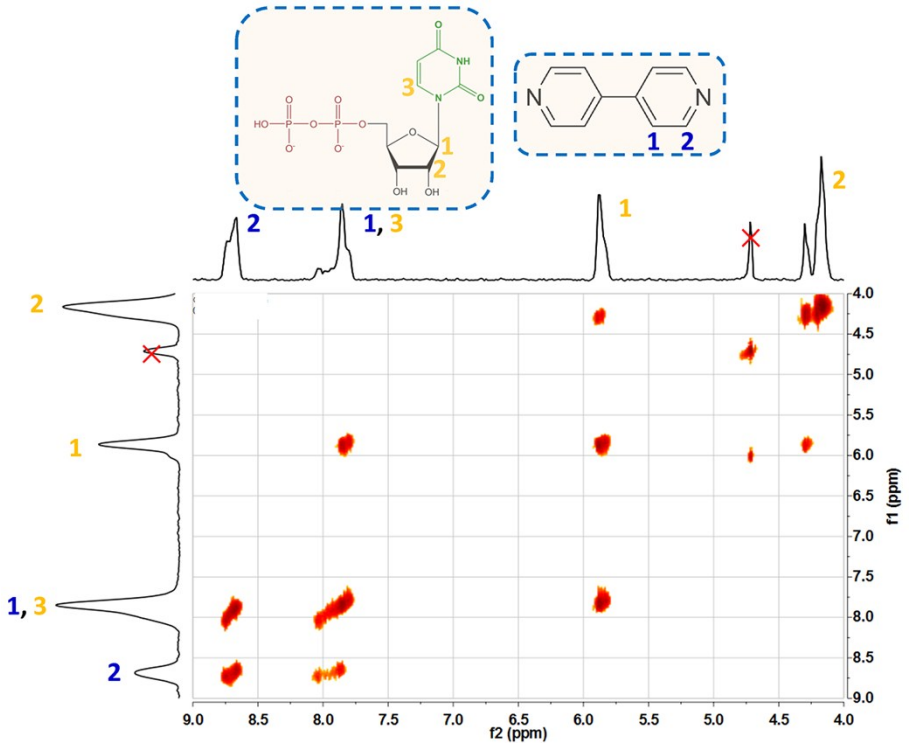


**Fig. S18.** 2D $^{1}$H-$^{1}$H COSY spectrum of Zn-UDP-4,4′-bipy in aqueous solution.

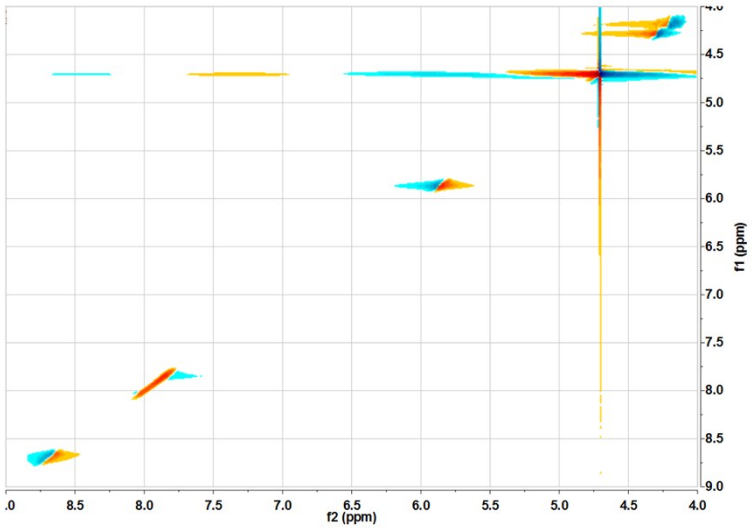


**Fig. S19.** 2D NOESY spectrum of Zn-UDP-4,4′-bipy in aqueous solution. There is no spatial coupling between hydrogen atoms in complex.

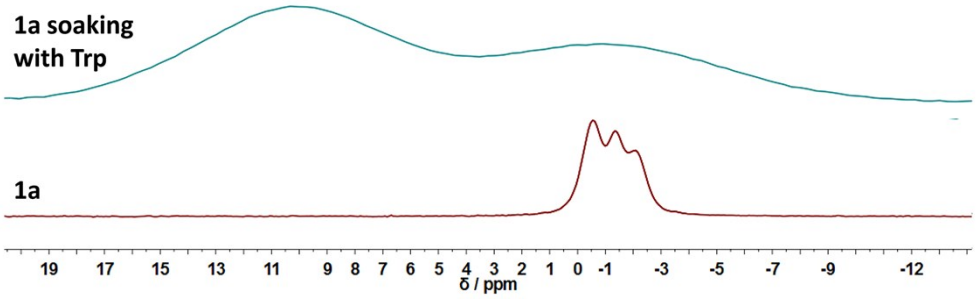


**Fig. S20.** Solid-state $^{31}$P NMR spectra of **1a** and **1a** after soaking with Trp.

## H. UV/vis Spectra

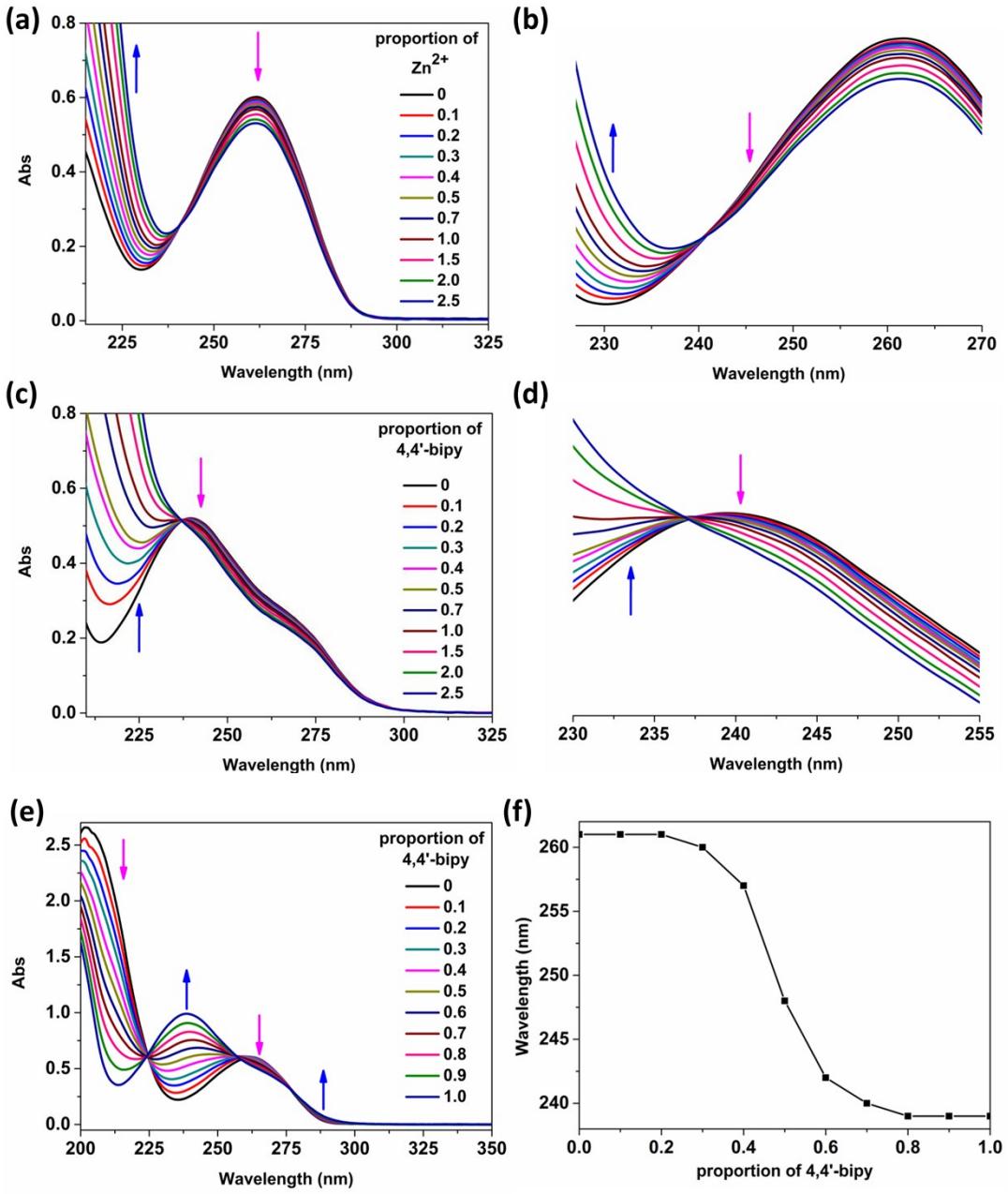


**Fig. S21** (a) UV/Vis spectroscopy titration of UDP upon addition of $Zn^{2+}$. The total concentration of UDP and $Zn^{2+}$ is $3.75 \times 10^{-5}$ mol·L$^{-1}$ varying the ratio of the components $Zn^{2+}$. (b) The isosbestic point around 242 nm is shown clearly. (c) UV/Vis spectroscopy titration of 4,4′-bipy upon addition of $Zn^{2+}$. The total concentration of 4,4′-bipy and $Zn^{2+}$ is $3.75 \times 10^{-5}$ mol·L$^{-1}$ varying the ratio of the components $Zn^{2+}$.(d) The isosbestic point around 237 nm is shown clearly. (e) UV/Vis spectroscopy titration of Zn-UDP upon addition of 4,4′-bipy. The total concentration of Zn-UDP and 4,4′-bipy is $3.75 \times 10^{-5}$ mol·L$^{-1}$ varying the ratio of the components 4,4′-bipy. (f) Plot of the complex formation of Zn-UDP with 4,4′-bipy, monitored with a UV/vis spectroscopy. All the spectra were obtained by measuring aqueous solution in a 1 cm cell.

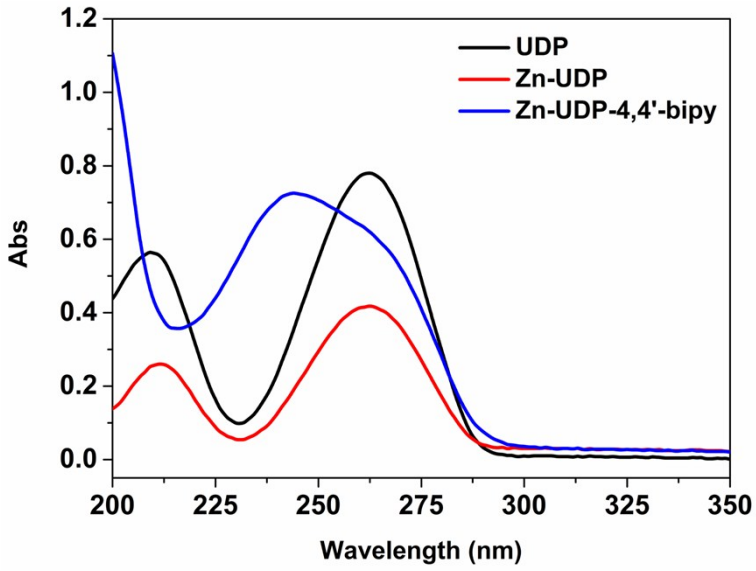


**Fig. S22.** UV/vis absorption spectra of UDP, Zn-UDP and Zn-UDP-4,4′-bipy in aqueous solution. The blue-shifts are observed in Zn-UDP-4,4′-bipy with respect to Zn-UDP after 4,4′-bipy was added. The spectra were obtained by measuring $5.0\times10^{-5}$ mol·L$^{-1}$ solution in a 1 cm cell.

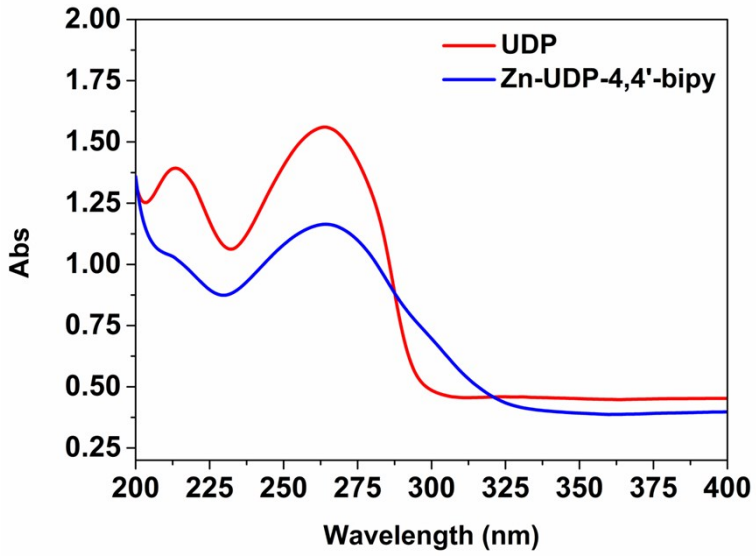


**Fig. S23.** The solid-state UV/vis absorption spectra of UDP and complex **1** at room temperature.

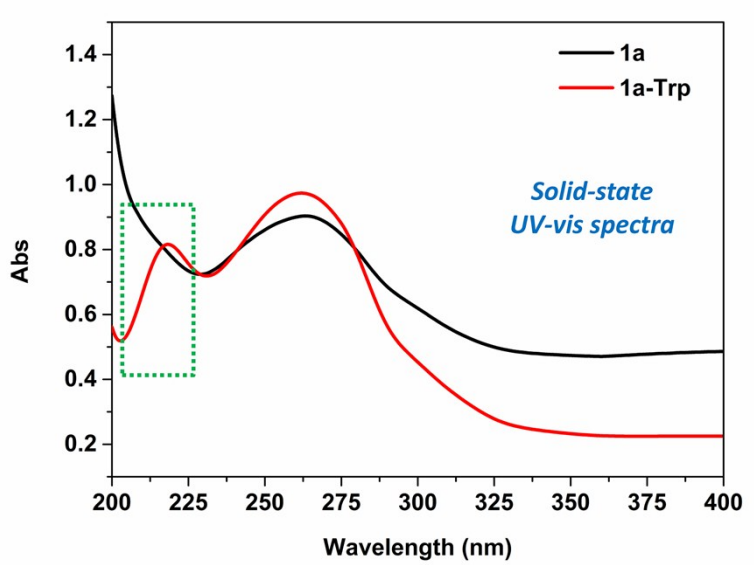


**Fig. S24.** Solid-state UV/vis spectra of complexes **1a** and **1a** after soaking with Trp amino acid in HEPES buffer (0.5 mM, pH = 7.4). The new absorption peak around 220 nm may indicate that Trp has interaction with **1a**.

# I. Fluorescence Emission Spectra of the Solution and Solid-State

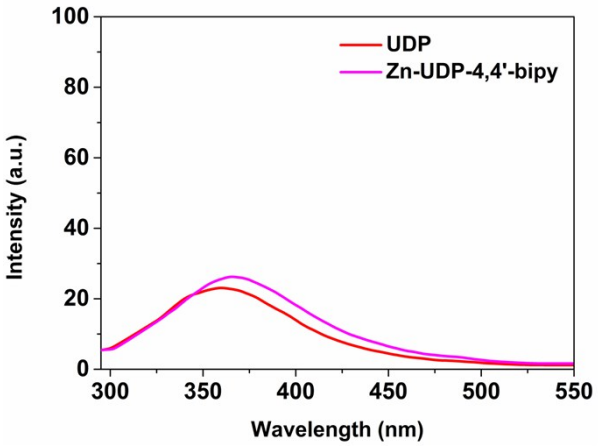


**Fig. S25.** Fluorescence emission spectra ($\lambda_{ex}$ = 280 nm) of the aqueous solution of UDP and Zn-UDP-4,4′-bipy. The spectra were obtained by measuring $5.0\times10^{-5}$ mol·L$^{-1}$ solution in a 1 cm cell and the slit width was 2.5 nm.

**Table. S5.** The solubility of as-synthesized **1** and activated **1a** in HEPES buffer (pH = 7.4).

| | as-synthesized (percentage of dissolution) | activated (percentage of dissolution) |
|---|---|---|
| in HEPES aqueous solution | 20% | 5% |

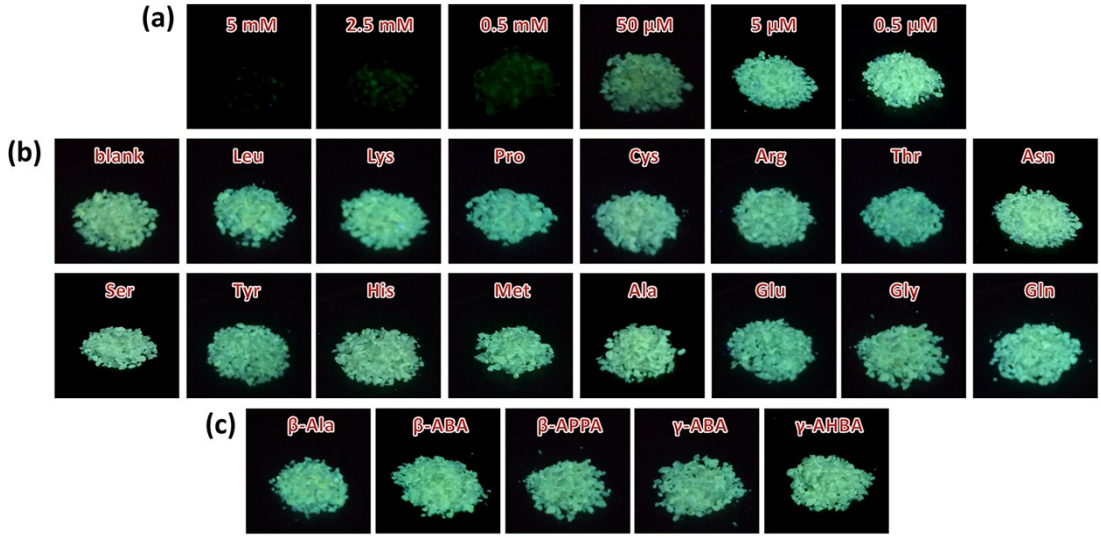


**Fig. S26.** (A) The images under UV-lamp of **1a** after soaking with Trp with different concentration in HEPES buffer (pH = 7.4); (B)The images under UV-lamp of **1a** after soaking with other 15 different α-amino acids (2.5 mM) in HEPES buffer (pH = 7.4); (C) The images under UV-lamp of **1a** after soaking with 5 different β-/γ-amino acids (2.5 mM) in HEPES buffer (pH = 7.4).

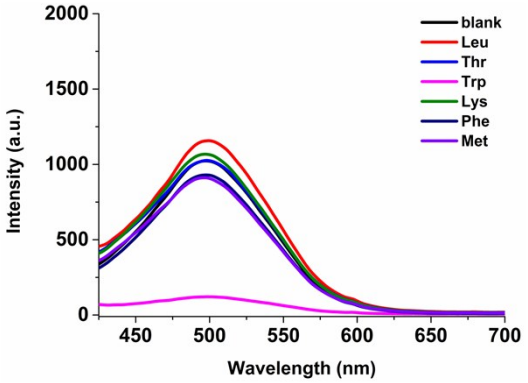


**Fig. S27.** Solid-state fluorescence emission spectra ($\lambda$ex = 335 nm) of **1a** after soaking with some essential amino acids in HEPES buffer (pH = 7.4). The slit width was 2.5 nm.

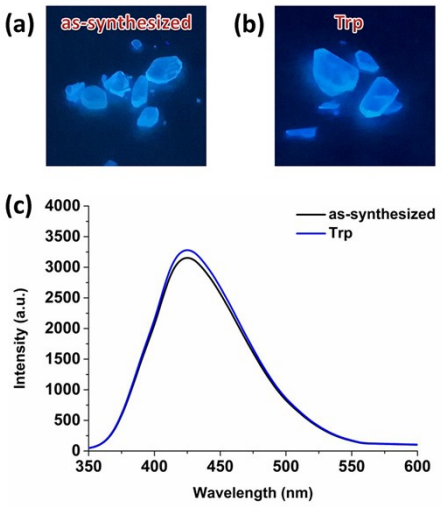


**Fig. S28.** (a, b) The images under UV-lamp of as-synthesized complex **1** and after soaking with tryptophan in HEPES buffer (pH = 7.4). (c) Solid-state fluorescence emission spectra ($\lambda$ex = 335 nm) of above two products. The slit width was 2.5 nm.

## J. CD Spectra

**Table S6.** Selected H-bonding distances (Å) and angles (°) for UDP and complex **1**.

| D–H | d(H···A) | ∠DHA | d(D···A) | A |
|---|---|---|---|---|
| **UDP** | | | | |
| N4–H10 (n) | 1.78 | 162 | 2.77 | O20 (αp ) |
| N2–H1 (n) | 1.88 | 173 | 2.90 | O8 (βp) |
| **Complex 1** | | | | |
| N6–H6 (n) | 1.91 | 174 | 2.79 | O3 (βp ) |
| N10–H10 (n) | 2.04 | 171 | 2.92 | O17 (βp) |

(αp) refers to α-oxygen on the phosphate group. (βp) refers to β-oxygen on the phosphate group. (n) refers to nucleobase.

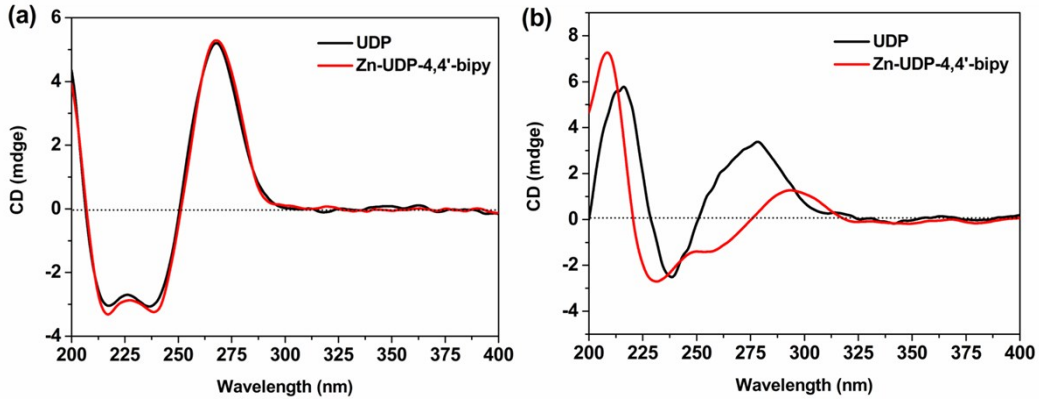


**Fig. S29.** (a) The CD spectra of the solution of UDP and complex **1**. The spectra was obtained by measuring $5.0\times10^{-5}$ mol·L$^{-1}$ solution in a 1 cm cell. In aqueous solution, a stronger and wider negative CD signal near 225 nm for UDP was attributed to n–π* and π–π* transitions. A positive signal near 268 nm was consistent with the UV/Vis spectrum, indicates that UDP is D-ribonucleotide. The CD spectra of UDP and its complex were similar, which indicates that the chirality in solution is mainly derived from the nucleotides. (b) The solid-state CD spectra of UDP and complex **1** (KBr : [sample] = 200 : 1). In the solid-state CD spectrum of UDP, three peaks were observed at 214, 239, and 279 nm, mainly caused by n–π* and π–π* transitions. In **1**, there are also three peaks. The positive signal centered at 209 nm and negative signal centered at 232m are attributed to the n–π* transition of the UDP ligand. These bands were blue-shifted compared to the UDP ligand. According to the analysis of the crystal structures of UDP, the H-bonding involved in uracil base is stronger than **1** (Table S6). The formation of stronger hydrogen bonds lower the system energy, so that the transition does not need to absorb higher energy and the CD bands in UDP are red-shifted compared with **1**. The positive peak near 295 nm was assigned to π–π* transition of the UDP ligand, which is red-shifted relative to the UDP ligand. In UDP, there was no π–π stacking interaction in the ligand (Fig. S1).[8–9] However, the extensive π–π stacking interactions between the nucleotide and 4,4'-bipy in the crystal lattice of **1** reduce the energy of the system (Figs. S5c, S7c), so that the π–π* transition does not need to absorb higher energy and the CD bands in complex are red-shifted (279 nm → 295 nm).

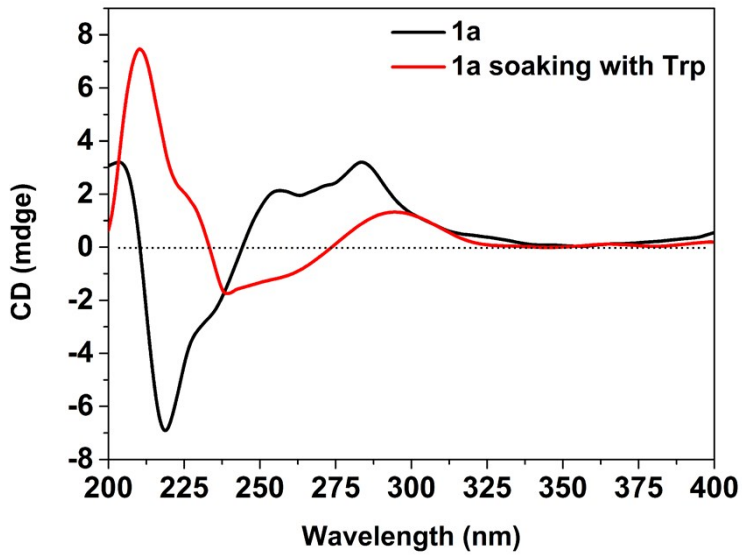


**Fig. S30.** The solid-state CD spectra of **1a** and **1a** soaking with Trp. (KBr : [sample] = 200 : 1).

## K. Thermogravimetric Analysis

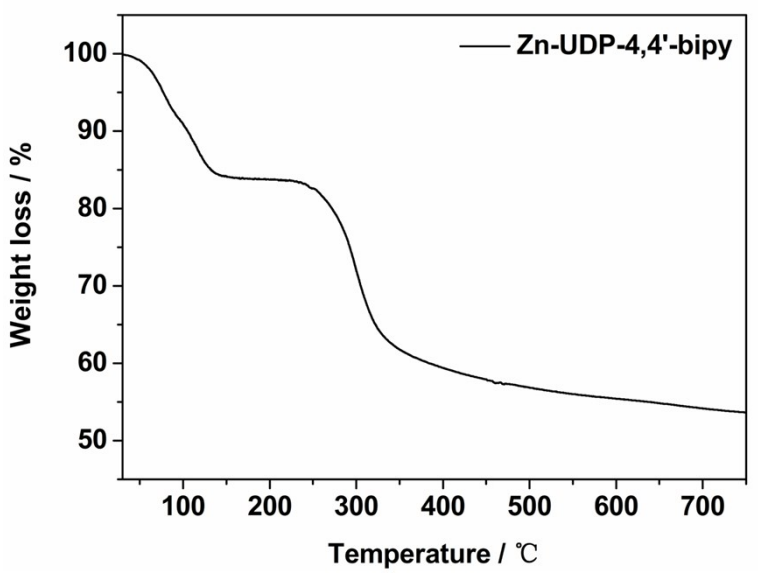


**Fig. S31.** TG curve of complex **1**. The TG curve of **1** shows a two-step weight loss process. The initial weight loss (**1**: obs. 16.0%, cal. 16.1%) in the temperature range 40–130°C is assigned to the loss of guest water solvates and coordinated water molecules per formula unit. The residue of complex begins to decompose around 245°C.

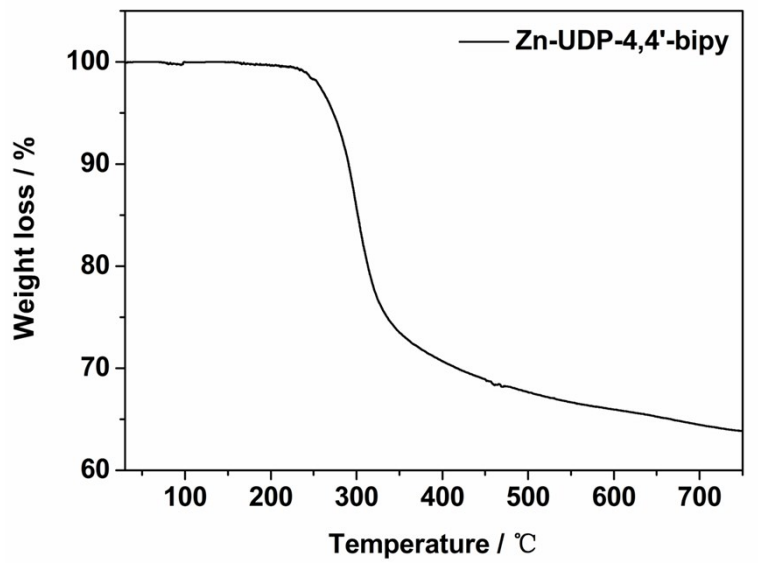


**Fig. S32.** TG curve of **1a**. The TG curve shows that the removal of all the coordinated and uncoordinated water molecules.

## L. References


[1] O. V. Dolomanov, L. J. Bourhis, R. J. Gildea, J. A. K. Howard and H. Puschmann, *J. Appl. Cryst.*, 2009, **42**, 339–341.

[2] G. M. Sheldrick, *Acta Cryst. C*, 2015, **71**, 3–8.

[3] M. A. Viswamitra, M. L. Post and O. Kennard, *Acta. Cryst. B*, 1979, **35**, 1089–1094.

[4] W. Sanger, Principles of Nucleic Acid Structure, *Springer*, *New York*, 1984.

[5] I. I. Comm., *Biochem.*, 1970, **9**, 3471–3479.

[6] W. Klyne and V. Prelog, *Experientia*, 1960, **16**, 521–523.

[7] I. I. Comm., *J. Org. Chem.*, 1970, **35**, 2849–2867.

[8] P. Zhou and H. Li, *Dalton Trans.*, 2011, **40**, 4834–4837.

[9] J. S. Ingwall, *J. Am. Chem. Soc.*, 1972, **94**, 5487–5495.